Evaluation of slowing down of proton and deuteron beams in CH_2, LiH, and Al partially ionized plasmas

David Casas, Manuel D. Barriga-Carrasco, and Juan Rubio
E.T.S.I. Industriales, Universidad de Castilla-La Mancha, E-13071 Ciudad Real, Spain
(Received 13 May 2013; published 9 September 2013)

In this work, proton and deuteron stopping due to free and bound electrons in partially ionized plasma targets is evaluated. The stopping of target free electrons is calculated using the dielectric formalism, well described in our previous works. In the case of target bound electrons, a short expression to calculate their contribution to the stopping is used, where mean excitation energies are obtained by means of the Hartree-Fock method. Experiments with different kinds of plasmas are analyzed. For LiH plasma, estimated plasma stopping fits experimental data very well, within the error bars, recognizing the well-known enhanced plasma stopping. In the case of CH_2 plasma, we obtain, from estimated ionization, that total stopping power increases when target electron density does. Our estimations are very similar to experimental data which show the same behavior with target free and bound electron density. Finally, in Al plasma, we compare directly our calculations with experimental data finding a very close agreement, where both stoppings have the same dependence on target ionicity. All these comparisons verify our theoretical model which estimates the proton or deuteron energy loss in partially ionized plasmas.

DOI: 10.1103/PhysRevE.88.033102 PACS number(s): 52.40.Mj, 52.65.Yy, 52.20.Fs, 52.25.Mq

I. INTRODUCTION

The stopping power of a free electron media, like plasmas, can be studied using dielectric formalism. In this theoretical frame, a classical or a quantum-mechanical linear response function known as the random phase approximation (RPA) is used [1,2]. This leads to considering the effect of the incident charged particle as a perturbation that loses energy on target proportionally to the square of its charge. The linear response theory is usually applicable for high-velocity projectiles and in the weak coupling of an electron gas. Then slowing down is simplified to a treatment of the properties of the medium only, and a linear description of these properties may then be applied.

In partially ionized plasmas, we must take into account the stopping power due to electrons bound to the target plasma atoms. This study can be performed using the mean excitation energy I that appears in the renowned expression of the Bethe logarithm

$$-\frac{dE}{dx} = \frac{4\pi Z_p^2 e^4 Z_a n_{at}}{m_e v^2} \ln \frac{2m_e v^2}{I}, \tag{1}$$

where Z_p and v are the projectile atomic number and velocity; Z_a and n_{at} are the target atomic number and density, respectively. This magnitude quantifies the energy exchanged in excitation and/or ionization processes of the electron shells. Mean excitation energy I can be determined through several methods such as the Hartree-Fock method (HF), oscillator strength (OS), or local plasma approximation (LPA).

In the literature, I has been calculated for every subshell of noble gases [3,4] and for all the elements from $Z_a = 1$ to $Z_a = 36$ [5]. Proton stopping in aluminum, nickel, argon, krypton, and xenon has been studied by means of generalized oscillator strength [6–8]. In general, these studies found values of I close to the ones obtained with available experiments or other theoretical calculations.

Mean excitation energy could be also estimated using LPA [9]. The LPA consists of averaging over density of the inhomogeneous fluid of bound electrons around a target ion. Then I could be determined using [10]

$$\ln I = Z_a^{-1} \int \ln[\gamma \hbar \omega_p(r)] \rho_b(r) d\vec{r} \tag{2}$$

with $\omega_p^2(r) = 4\pi\rho_b(r)e^2/m_e$ and $\gamma = \sqrt{2}$, where $\rho_b(r)$ is the bound electron radial density. A simple analytic formula for I was proposed through a variational method, $I = \sqrt{2K/\langle r^2 \rangle}$.

The aim of this work is to analyze the slowing down of projectiles with $Z_p = 1$ (protons and deuterons) in different partially ionized plasmas. The existence of free and bound electrons in plasma implies that both must be considered for calculation of stopping. For this, the paper is divided into three main sections. In Sec. II, it is shown how the electronic stopping is calculated. First, the calculation of stopping power of target free electrons is estimated using the RPA dielectric function. Later it is shown how to estimate the stopping power of target bound electrons by means of mean excitation energy I, and how this I is obtained. Then in Sec. III, it is explained how the Hartree-Fock method works in order to obtain the mean excitation energy for any atom or ion of plasma target. Finally in Sec. IV, we analyze three different experiments of slowing down of ions in plasmas using the electronic stopping methods shown in Sec. II. We will use atomic units (a.u.), $e = \hbar = m_e = 1$, to simplify formulas.

II. ELECTRONIC STOPPING

A. Electronic stopping due to free electrons

The RPA dielectric function (DF) is developed in terms of the wave number k and of the frequency ω provided by a consistent quantum mechanical analysis. The RPA analysis yields the expression [11]

$$\epsilon_{\mathrm{RPA}}(k,\omega) = 1 + \frac{1}{\pi^2 k^2} \int d^3k' \frac{f(\vec{k}+\vec{k}') - f(\vec{k}')}{\omega + iv - (E_{\vec{k}+\vec{k}'} - E_{\vec{k}'})}, \tag{3}$$

where $E_{\vec{k}} = k^2/2$. The temperature dependence is included through the Fermi-Dirac function

$$f(\vec{k}') = \frac{1}{1+\exp[\beta(E_k-\mu)]}, \tag{4}$$

with $\beta = 1/k_B T$ and μ the chemical potential of the plasma with electron density n_e and temperature T. In this part of the analysis we assume the absence of collisions so that the collision frequency tends to zero, $v \to 0$.

The analytic RPA DF for plasmas at any degeneracy can be obtained directly from Eq. (3) [12,13]:

$$\epsilon_{\mathrm{RPA}}(k,\omega) = 1 + \frac{1}{4z^3\pi k_F}[g(u+z) - g(u-z)], \tag{5}$$

where $g(x)$ corresponds to

$$g(x) = \int_0^\infty \frac{y\,dy}{\exp(Dy^2-\beta\mu)+1} \ln\left(\frac{x+y}{x-y}\right);$$

$u = \omega/kv_F$ and $z = k/2k_F$ are the common dimensionless variables [11]. $D = E_F\beta$ is the degeneracy and $v_F = k_F = \sqrt{2E_F}$ is Fermi velocity in a.u.

Finally, electronic stopping of free plasma electrons will be calculated in the dielectric formalism as

$$S_f(v) = \frac{2Z_p^2}{\pi v^2}\int_0^\infty \frac{dk}{k}\int_0^{kv} d\omega\omega\,\mathrm{Im}\left[\frac{-1}{\epsilon_{\mathrm{RPA}}(k,\omega)}\right](\text{a.u.}),$$

where Z_p is the charge, v is the velocity of the projectile, and the equation is in atomic units.

B. Electronic stopping due to bound electrons

In order to determine electronic stopping due to bound electrons we use analytical formulas in the limit of low and high projectile velocities, and an interpolating expression is derived for intermediate velocities. For a plasma target with atomic density n_{at}, the bound electron density for each populated atomic shell is $n_i = P_i n_{at}$, where P_i is the average electron population in the shell of a target atom [14]. We can estimate electronic stopping for a proton beam in the form

$$S_b = \frac{4\pi n_{at}}{v^2}(L_b + L_K), \tag{6}$$

where L_K is the Barkas stopping number defined in [15],

$$L_K = Z_p\frac{1.7\lambda_{\mathrm{eff}}}{v^2}\ln\frac{2v}{\lambda_{\mathrm{eff}}},$$

and $\lambda_{\mathrm{eff}} = 0.72Z_a^{1/3}$. On the other hand,

$$L_b = \sum_i P_i L_i, \tag{7}$$

where L_b is the stopping number for whole bound electrons of atom or ion and L_i is the stopping number for bound electrons of each shell.

We reckoned L_b by interpolating between the asymptotic formulas valid either for low or for high projectile velocities [16],

$$L_b(v) = \begin{cases} L_H(v) = \ln\frac{2v^2}{I} - \frac{2K}{v^2} & \text{for} \quad v > v_{\mathrm{int}}, \\ L_B(v) = \frac{\alpha v^3}{1+Gv^2} & \text{for} \quad v \leqslant v_{\mathrm{int}}, \end{cases} \tag{8}$$

$$v_{\mathrm{int}} = \sqrt{3K + 1.5I}, \tag{9}$$

where G is given by $L_H(v_{\mathrm{int}}) = L_B(v_{\mathrm{int}})$, K is the electron kinetic energy, I is the mean excitation energy, and α is the friction coefficient for low velocities. The mean excitation energy of each shell is determined using

$$I = \sqrt{\frac{2K}{\langle r^2\rangle}}, \tag{10}$$

where $\langle r^2\rangle$ is the average of the square of the radius, for the electron in the i shell. Within the hydrogenic approximation, the friction coefficient of each shell is given by $\alpha = 1.067\sqrt{K}/I$ [10].

Equation (10) is obtained within the framework of oscillator strength. It is defined by

$$f_{0n} = \frac{2E_{0n}}{N}\langle n|\sum_{i=1}^{N} z_i|0\rangle, \tag{11}$$

where the excitation energy is E_{0n}, calculated for transitions $0 \to n$ in a given atom or ion with N bound electrons, and the nuclear charge is Z_a.

The momenta $S(\mu)$ and $L(\mu)$ are calculated using the oscillator strength sum rules [17]

$$S(\mu) = \sum_n f_{0n}E_{0n}^{\mu}, \tag{12}$$

$$L(\mu) = \sum_n f_{0n}E_{0n}^{\mu}\ln|E_{0n}|. \tag{13}$$

When $\mu = -1$

$$S(-1) = \frac{2m_e}{3\hbar^2}a_0^2\left\langle\left(\frac{r}{a_0}\right)^2\right\rangle, \tag{14}$$

then $S(-1)$ is proportional to square radius. If atomic units are used it is reduced to the expression

$$\langle r^2\rangle = \tfrac{3}{2}S(-1). \tag{15}$$

Substituting $\mu = 1$ in Eq. (12), an expression proportional to the kinetic energy is obtained,

$$S(1) = \frac{4}{3}\langle 0|\frac{p^2}{2m_e}|0\rangle, \tag{16}$$

using atomic units

$$2K = \tfrac{3}{2}S(1). \tag{17}$$

The quantity $L(0)$ is related with the mean excitation energy I,

$$\ln I = \frac{L(0)}{S(0)} = \frac{L(0)}{N}; \tag{18}$$

moreover, $\ln I$, $S(0)$, $S(1)$, and $S(-1)$ are related by [10]

$$\ln I = \frac{1}{2}\ln\left[\frac{S(1)}{S(-1)}\right]. \tag{19}$$

Substituting Eqs. (15) and (17) in Eq. (19) the expression (10) is achieved.

Using Eq. (10) we can easily estimate I from the atomic parameters K and $\langle r^2\rangle$. In the next section we will explain how to obtain these quantities from Hartree-Fock calculations [18].

III. HARTREE-FOCK METHOD

To obtain the atomic parameters K and $\langle r^2\rangle$ we need to solve the Schrödinger equation for the bound electrons of the atom. But only for the hydrogen atom or hydrogen-like atoms are there analytical solutions of this equation. However, there are no exact solutions for atoms with more than one electron; for this reason we must use other approximating methods to estimate the atomic properties of many-electron atoms. The well-know Hartree-Fock method simplifies the many-electron problem to a one-electron problem, where each electron moves in an effective potential which takes into account the attraction of the nucleus and the average effect of the repulsive interactions due to the other electrons. This method also obeys the Pauli exclusion principle due to the fermionic nature of electron.

The Hartree-Fock equations for an electron i with coordinate $\mathbf{R}_i$ is

$$\left[-\frac{1}{2}\nabla_i^2 - \frac{Z}{r_i} + V_i(\mathbf{r}_i)\right]\Psi_{Q_i}(\mathbf{R}_i) - \sum_{\substack{j\\ j\neq i}} \int \frac{\Psi^*_{Q_j}(\mathbf{R}_j)\Psi_{Q_i}(\mathbf{R}_j)}{|\mathbf{r}_i - \mathbf{r}_j|} d\tau_j \cdot \Psi_{Q_i}(\mathbf{R}_i) = E\Psi_{Q_i}(\mathbf{R}_i), \tag{20}$$

where the first term in the bracket is the kinetic energy, the second the potential energy due to the nucleus, the third the Coulomb interaction energy with all the other electrons, and the last term of the first member is called the exchange term, which includes the antisymmetry of the wave function [19,20].

Furthermore the wave function of the one electron could be expressed with all its quantum numbers, including spin [21],

$$\Psi_{Q_j}(\mathbf{R}_j) = R_{nl}(\mathbf{r}_j)Y_{lm_l}(\theta,\phi)X_{m_s}(\sigma_j). \tag{21}$$

From Eq. (21) are obtained kinetic energy and mean square radius in order to solve the expression $I = \sqrt{2K/\langle r^2\rangle}$. We estimate K and $\langle r^2\rangle$ through the integration of the following radial functions:

$$K_{nl} = -\frac{1}{2}\int_0^\infty P_{nl}(r)\left[\frac{d^2}{dr^2} - \frac{l(l+1)}{r^2}\right]P_{nl}(r)dr, \tag{22}$$

where

$$R_{nl}(r) = \frac{1}{r}P_{nl}(r), \tag{23}$$

satisfying normalization condition [21],

$$\int_0^\infty P^2_{nl}(r)dr = 1. \tag{24}$$

The general formula to obtain mean powers of radius is [19]

$$\langle r^p\rangle_{nml} = \int_0^\infty |R_n l(r)|^2 r^{p+2}dr, \tag{25}$$

TABLE I. Atomic quantities in a.u. for neon.

Neon	Hartree-Fock			Oscillator Strength		
Shell	K	$\langle r^2\rangle$	I	K	$\langle r^2\rangle$	I
$1s$	46.269	0.033	52.954	42.837	0.013	81.621
$2s$	5.214	0.967	3.284	4.901	0.076	11.363
$2p$	4.264	1.228	2.635	3.151	1.428	2.101

substituting 2 instead of p in this particular case. These equations are solved for any atom using a FORTRAN 95 code [22] including K and $\langle r^2\rangle$.

In Table I we can see the different atomic quantities calculated for neon using Hartree-Fock and oscillator strengths. For all subshells, when the principal quantum number n rises, the mean excitation energy and electron kinetic energy of each subshell decreases while mean quadratic radius increases. The values corresponding to the oscillator strength calculations are obtained from Eqs. (10), (15), and (17). The quantities related to $S(1)$ and $S(-1)$ are tabulated in [4].

IV. RESULTS

In this section we will evaluate the stopping power of three different types of plasmas: LiH, CH_2, and Al. The electron kinetic energy, mean quadratic radius, and mean excitation energy of atomic subshells are shown in Table II for each plasma target. K and $\langle r^2\rangle$ are calculated by mean of the Hartree-Fock method and I using Eq. (10). These quantities vary in the same way as those in Table I.

A. LiH plasma

There are only a few experiments on beam plasma interaction in low beam energies, below 0.5 MeV. In this experiment, a proton beam interacts with lithium hydride plasma. This was produced by irradiating a small pellet (diameter ≈ 60 μm) of LiH with a Q-switched Nd-glass laser ($\lambda = 1054$ nm). The energy loss by a proton beam, with initial energy of 350 keV ($v \approx 3.7$ a.u.), was measured after passing through the plasma. By spectroscopic analysis, temperature and electron density were measured at 60 ns after the laser was fired and these were 20 eV and 10^{18} e^-/cm^3, respectively. The

TABLE II. Atomic quantities in a.u. for each subshell of plasma elements.

Element	Subshell	K	$\langle r^2\rangle$	I
H	$1s$	0.500	3.000	0.577
Li	$1s$	3.612	0.447	4.021
	$2s$	0.209	17.738	0.153
C	$1s$	16.053	0.097	18.176
	$2s$	1.546	3.038	1.009
	$2p$	1.230	3.890	0.795
Al	$1s$	79.264	0.019	90.257
	$2s$	10.884	0.459	6.887
	$2p$	9.856	0.455	6.579
	$3s$	0.936	7.891	0.487
	$3p$	0.571	14.006	0.286

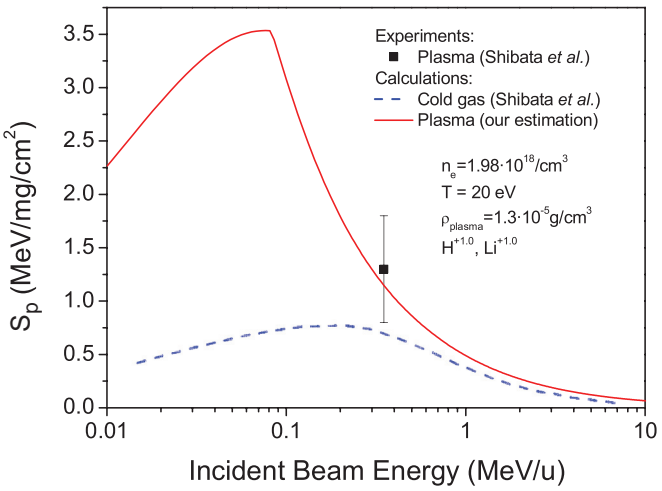

FIG. 1. (Color online) Proton stopping in a LiH plasma as a function of beam energy. Shibata *et al.*: Squares, experiments in plasma; dashed curve, calculations in cold gas. Our work: Solid curve, calculations in plasma.

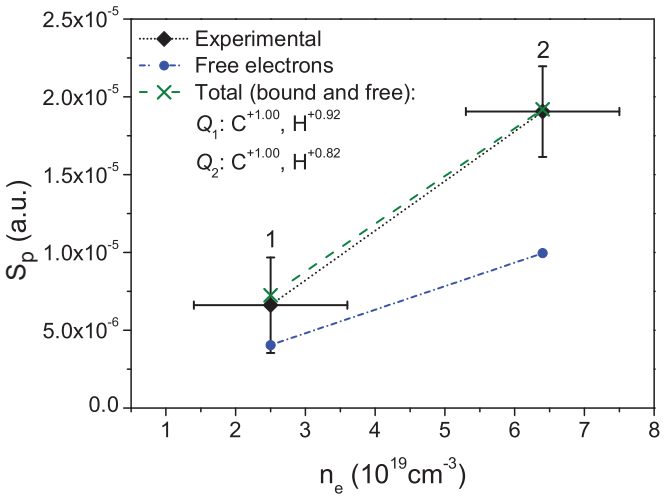

FIG. 2. (Color online) Proton stopping as a function of CH_2 plasma electron density. Experimental: Diamonds. Calculated: Circles, free electrons; crosses, total.

mass thickness ($\Delta\rho x$) was 1.3 μg/cm^3 [23] so it is possible to determine plasma density with the plasma length, $\Delta x =$ 0.1 cm, measured previously [24]. Then, we find the plasma density, $\rho_{\text{plasma}} = 1.3\ \mu\text{g/cm}^2/0.1\ \text{cm} = 1.3 \times 10^{-5}\ \text{g/cm}^3$ and the same atomic density for lithium and hydrogen is obtained, $n_{at} = 9.88 \times 10^{17}$ at./cm^3. The ionization is also the same for both, $q_{\text{Li}} = q_{\text{H}} = +1.0$, and it was calculated by those authors using the Saha equation for this kind of plasma [25–28].

Figure 1 shows the experimental stopping of the cold equivalent and plasma, and our calculations. Our estimation for the plasma case is very close to the experimental datum point. At low beam energies, the stopping is much higher for plasma than for cold gas while for high beam energies, the difference is negligible. This behavior is known as enhanced plasma stopping and is due to the influence on stopping of the higher free electron density in plasmas.

B. CH_2 plasma

The plasma was created from a polyethylene plastic, $[CH_2]_n$, using an electric discharge. The energy loss of a 3 MeV proton beam ($v \approx 11$ a.u.) was measured after passing through a plasma column 50 mm long [29]. With the energy loss ΔE and the plasma length Δx, it is possible to estimate the experimental stopping power, $S_p = \Delta E/\Delta x$.

In this experiment the free electron density n_f was measured, but not the ionic density or the ionization degree. We have calculated the ionization for hydrogen using the Saha equation. In the case of carbon, the authors estimated that there are five bound electrons for the plasma target [30]. The temperature, energy loss, and ionization are placed in Table III.

Figure 2 compares calculated stopping of free and total electrons with the same experimental data with error bars. The difference between both is caused by the stopping of bound electrons. In addition, we include the total stopping (bound and free) using the ionization for carbon and hydrogen shown in Table III. Stopping rises when the electron density rises because the ionization is approximately the same and rest of the variables remain constant. Our calculations are very close to the experimental results.

C. Aluminum plasma

In this section, we compare our methods with experimental data of aluminum plasmas [31]. In this experiment, the energy loss of deuterons in plasmas is measured. A pinch-reflex diode produces the deuteron beam. The plasma target is placed at the center of cathode and is enclosed between two deuterated polyethylene (CD_2) foils. Aluminum is used to produce the plasma target.

The anode has a CD_2 foil that provides the deuteron beam. This beam reaches 1 MeV in 4 cm (the distance between anode and cathode). A spherical anode is used for the experiments. In Table IV, we can see the conditions of the plasma target for each case.

Time of flight (ToF) of neutrons with multilayered targets is used to determine deuteron energy loss. Neutrons come from the foils that enclosed the plasma target. Using neutron incident energy, deuteron energy loss in the plasma target is calculated.

TABLE III. Energy loss and plasma parameters.

Case i	ΔE (keV)	T_e (eV)	n_f (10^{19} e^-/cm^3)	H ionization	C ionization
1	170 ± 79	3.3 ± 0.3	2.5 ± 1.1	+0.92	+1.0
2	490 ± 75	3.3 ± 0.3	6.4 ± 1.1	+0.82	+1.0

TABLE IV. Experimental conditions of aluminum plasma [31].

T (eV)	n_e (10^{21} e^-/cm^3)	Q
13–17	1.50	3.37
13–17	1.56	3.49
13–17	1.91	4.27

In this experiment, it was proposed that stopping power with target ionization can be formulated as [31]

$$S_p = B\left[1 - \frac{Q}{Z_a}L_b + \frac{Q}{Z_a}L_f\right], \tag{26}$$

where Q is the mean ionization and Z_a is the atomic number of the target,

$$B = \frac{4\pi Z_a n_{at}}{v^2}, \tag{27}$$

where v is the projectile velocity. The parameters L_b and L_f are, respectively,

$$L_b = \ln\frac{2v^2}{I_b}, \tag{28}$$

$$L_f = \ln\frac{2v^2}{I_f}, \tag{29}$$

where

$$I_b \simeq \bar{I}_I(Q) = \left(\frac{Z_a}{Z_a - Q}\right)^2 \bar{I}_N(Z_a - Q) \tag{30}$$

and

$$I_f = \omega_p. \tag{31}$$

In Eq. (30) the term $\bar{I}_I(Q)$ is the average of the mean excitation energy of the target ion, while $\bar{I}_N(Z_a - Q)$ is the average of the mean excitation energy of the neutral atom with atomic number $Z_a - Q$ [32]. In Eq. (31) ω_p is the plasma frequency.

We compare our calculations with the measurements in Fig. 3. We show three experiments with their temperature, electron density, and ionicity. Experimental data have high uncertainty because deuterons impact on the target with a large range of angles [31]. Their estimations are based on hydrocode calculations, while ours are based on Hartree-Fock method. In all cases, our results are within experimental data error bars, having more accuracy for the highest ionization case. The three theoretical curves show a dependence with ionicity and incident deuteron energy. When the ionicity rises the energy loss also does, but when the incident deuteron energy rises the energy loss decreases. This behavior is also observed in the experimental points. The difference in energy loss for the two cases with similar incident energy, near 0.5 MeV/u, is due mainly to the difference in plasma ionization. The case with the highest ionization, 3.49, shows a higher energy loss than the case with ionization 3.37, due to the higher free electron density of the former. The third case shows a lower energy loss compared with the two first ones, although its ionicity is higher, 4.27, because the incident energy is higher, by 0.6 MeV/u. In conclusion, our theoretical estimations show the same relationship between energy loss, ionicity, and incident deuteron energy as the experimental data. Furthermore, the stopping power calculated is within the experimental data error bars. Finally for the highest ionization, there is a good agreement between our calculation, the experimental data point, and the theoretical estimation from [31].

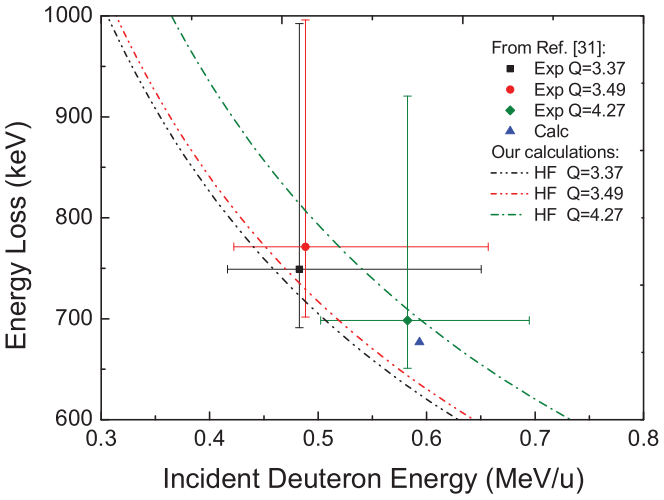

FIG. 3. (Color online) Energy loss of deuterons in aluminum plasma for different target ionizations. Experimental data (exp. made with spherical anode), calculations (Calc) from [31]; and our estimation (HF). Free and bound target electrons are considered.

V. CONCLUSIONS

In this work, the energy loss of proton and deuteron beams in plasmas caused by the stopping power of free and bound electrons was analyzed by means of the RPA dielectric function and Hartree-Fock method, respectively. We have compared our calculations with experimental data obtained from different partially ionized plasma targets.

For LiH plasma we have obtained the plasma density. Using the ionization of Li and H, given by the authors, we were able to obtain the stopping of bound and free electrons. With this ionization, our estimation fell within the experimental error bars. The enhanced plasma stopping comparing cold matter to the plasma state was also shown.

Proton stopping was measured in CH_2 plasmas with the result that free electrons caused a considerable part of stopping power and the remaining part was due to bound electrons. Because hydrogen was highly ionized and carbon lost one electron only, the main contribution to stopping of bound electrons was due to the latter one. Using both ionizations, we have estimated total stopping and we have found that it increases when the electron density rises. Our calculated slowing down was very close to experimental measures that showed the same dependence with electron density.

Finally, the total stopping power of the deuteron beam in aluminum plasma was calculated for different ionizations and beam energies. Our calculations show the same dependence of energy loss with ionicity and incident energy as the experimental cases. In addition, the estimated energy loss

was within the experimental data error bars with the best adjustment for the highest ionization.

These good results verify our theoretical model that estimates the proton or deuteron energy loss in partially ionized plasmas.

ACKNOWLEDGMENTS

We are particularly grateful to M. A. Mendoza and J. G. Rubiano for their continuous strong support of the calculations. This work was financed by the Spanish Ministerio de Ciencia e Innovación (under contract No. ENE2009-09276).

[1] M. D. Barriga-Carrasco, Phys. Rev. E **76**, 016405 (2007).
[2] M. D. Barriga-Carrasco, Phys. Rev. E **82**, 046403 (2010); Laser Part. Beams **28**, 307 (2010); **29**, 81 (2011).
[3] R. J. Bell and A. Dalgarno, Proc. Phys. Soc. **89**, 55 (1966).
[4] R. J. Bell, D. R. B. Bish, and P. E. Gill, J. Phys. B: At. Mol. Phys. **5**, 476 (1972).
[5] D. E. Meltzer, J. R. Sabin, and S. B. Trickey, Phys. Rev. A **41**, 220 (1990).
[6] E. J. McGuire, J. M. Peek, and L. C. Pitchford, Phys. Rev. A **26**, 1318 (1982).
[7] E. J. McGuire, Phys. Rev. A **28**, 2096 (1983).
[8] E. J. McGuire, J. Appl. Phys. **70**, 7213 (1991).
[9] J. Lindhard and M. Scharff, K. Dan. Vidensk. Selsk. Mat. Fys. Medd. **27**, 15 (1953).
[10] X. Garbet, C. Deutsch, and G. Maynard, J. Appl. Phys. **61**, 907 (1987).
[11] J. Lindhard, K. Dan. Vidensk. Selsk. Mat. Fys. Medd. **28**, 8 (1954).
[12] C. Gouedard and C. Deutsch, J. Math. Phys. **19**, 32 (1978).
[13] N. R. Arista and W. Brandt, Phys. Rev. A **29**, 1471 (1984).
[14] M. D. Barriga-Carrasco and G. Maynard, Laser Part. Beams **23**, 211 (2005).
[15] I. Nagy, Phys. Rev. A **65**, 014901 (2001).
[16] G. Maynard and C. Deutsch, J. Phys. (Paris) **46**, 1113 (1985).
[17] U. Fano and J. W. Cooper, Rev. Mod. Phys. **40**, 441 (1968).
[18] C. F. Fischer, Comput. Phys. Commun. **43**, 355 (1987).
[19] B. H. Bransden and C. J. Joachain, *Physics of Atoms and Molecules* (Logman Scientific & Technical, New York, 1983), p. 320–327.
[20] H. Haken and H. C. Wolf, *The Physics of Atoms and Quanta* (Springer, Berlin, 2005), pp. 355–358.
[21] C. F. Fischer, T. Brage, and P. Jönsson, *Computational Atomic Structure: An MCHF Approach* (Institute of Physics Publishing, Bristol, 1997), pp. 9, 42.
[22] C. F. Fischer and G. Tachiev, http://nlte.nist.gov/MCHF
[23] K. Shibata *et al.*, Nucl. Instrum. Methods Phys. Res. Sect. A **464**, 225 (2001).
[24] Y. Oguri *et al.*, Nucl. Instrum. Methods Phys. Res. Sect. A **415**, 657 (1998).
[25] A. Sakumi *et al.*, J. Nucl. Sci. Tech. **36**, 326 (1999).
[26] K. Shibata *et al.*, Nucl. Instrum. Methods Phys. Res. Sect. B **161**, 106 (2000).
[27] A. Sakumi *et al.*, Nucl. Instrum. Methods Phys. Res. Sect. A **464**, 231 (2001).
[28] M. Ogawa *et al.*, Nucl. Instrum. Methods Phys. Res. Sect. A **464**, 72 (2001).
[29] A. Golubev *et al.*, Phys. Rev. E **57**, 3363 (1998).
[30] A. Golubev *et al.*, Nucl. Instrum. Methods Phys. Res. Sect. A **464**, 247 (2001).
[31] F. C. Young, D. Mosher, S. J. Stephanakis, and S. A. Goldstein, Phys. Rev. Lett. **49**, 549 (1982).
[32] T. A. Mehlhorn, J. Appl. Phys. **52**, 6522 (1981).